Journal of High School Science

Cell-type-specific chromatin accessibility patterns in aging hippocampal neural stem cells reveal MEF2 family motif enrichment

Chae N

Submitted: December 21, 2025, Revised: version 1, January 22, 2026, version 2, January 23, 2026
Accepted: January 26, 2026

Abstract

The mammalian brain continues to generate new neurons throughout life. This regenerative potential is dependent on neural stem cell pools and declines with age or in neurodegenerative diseases, contributing to memory impairment and cognitive decline. Although epigenetic remodeling has been implicated in neural stem cell aging, transcriptional features associated with this process remain incompletely characterized. Previously generated publicly available ATAC (Assay for Transposase-Accessible Chromatin)-seq datasets were analyzed to identify age-associated chromatin accessibility patterns in hippocampal neural stem cells. Using peak presence-based comparisons, genomic regions were identified as accessible in older samples but not in younger counterparts under consistent peak-calling thresholds. Motif enrichment analysis of these regions revealed overrepresentation of MEF2 family binding motifs alongside reduced representation of motifs associated with neurogenic transcription factors. Complementary analysis of independent gene expression datasets showed increased MEF2C transcript levels in aged hippocampal neural stem cells. An exploratory *in vitro* overexpression assay in a human neural progenitor-like cell line revealed altered cell morphology and reduced cell-cell contact. Importantly, the MEF2-family motif enrichment was observed selectively in hippocampal neural stem cell peak sets and was not detected in whole hippocampal tissue or subventricular zone neural stem cell datasets, demonstrating that aging-associated chromatin features are strongly cell-type dependent. Together, these findings identify MEF2C as a candidate gene associated with aging-related chromatin features in hippocampal neural stem cells and generate hypotheses for future functional studies.

Keywords

Brain aging, Hippocampal neurogenesis, Neural stem cells, Transcription factors, Chromatin accessibility, Cell-cell contact, Myocyte Enhancer Factor 2C (MEF2C), Neurodegenerative disease, Epigenetic remodeling, Cognitive decline

Nathaniel Chae, Stuyvesant High School, 345 Chambers St, New York, NY10282, USA. chaenathaniel@gmail.com

https://doi.org/10.64336/001c.155781

1. Introduction

The socioeconomic impact of aging populations has become globally significant (1). The loss of cognitive functions such as learning and memory is part of the natural process of aging. However, this decline often accompanies depression and other negative emotional effects in aging populations, which are increasingly recognized as major societal issues.

The mammalian brain continues to produce neurons during aging and injury (2). This capacity is rooted in the pool of neural stem cells in the brain. The hippocampus is the site of continued production of neurons, unlike other regions of the brain (2, 3). Adult hippocampal neurogenesis has been shown to play a critical role in maintaining cognitive functions in response to aging and its associated neurodegenerative conditions such as Alzheimer's disease and Parkinson's disease (4-6).

Hippocampal neurogenesis declines with age (7). However, external factors such as physical activity (8-10) and nutrition (11) have been shown to slow this decline and have been associated with improved cognitive outcomes in humans and experimental animal models. For instance, exercise promotes the expression of neurotrophic factors like Brain-Derived Neurotrophic Factor (BDNF), which is essential for neural stem cell homeostasis and facilitating neuroplasticity (12). Unfortunately, the molecular mechanisms which cause hippocampal neurogenesis to decline in the aging brain remain to be identified.

Efforts to molecularly define cellular aging led to the development of the theory of 'epigenetic clocks' (13). DNA methylation has been shown to exhibit age-correlated patterns across tissues and species, allowing fairly accurate prediction of both chronological and biological age (13-15). Among those epigenetically modified genes, increased DNA methylation in developmental cell fate genes suggests that the aging process may suppress the expression of specific genes (15). Additionally, chromatin accessibility and nucleosomal landscape changes have been reported to be associated with aging in various tissue types (16-19). More recent studies have shown that developmental cell-type identity defining transcription factors reduce chromatin accessibility during aging. Conversely, activator protein 1 (AP-1) transcription factors, which are activated by stress stimuli including injury and inflammatory signaling in aging tissues are increasingly represented in accessible chromatin regions (20). These studies suggest that transcriptional changes induced by transcription factor redistribution and coordinated by age-related chromatin accessibility may contribute to cellular and organismal aging. Despite these advances, the transcriptional and epigenetic mechanisms underlying hippocampal neural stem cell aging and approaches to mitigate their functional decline in the aging brain remain to be investigated. However, whether aging-associated chromatin features reflect shared regulatory programs across neural tissues or instead arise in a cell-type–specific manner remains unclear.

In the present study, age-associated changes in regulatory features were hypothesized to be reflected in the chromatin peak landscapes of hippocampal neural stem cells. To test this, multiple publicly available Assay for

Transposase-Accessible Chromatin sequencing (ATAC-seq) datasets were analyzed to identify transcription factor sequence motifs selectively represented in hippocampal neural stem cells from old and aged mice. In addition, the potential function of Myocyte Enhancer Factor 2C (MEF2C), which emerged as a candidate from motif enrichment and expression analyses, was explored.

This study takes an unbiased approach to identify previously unexplored molecular changes within aging hippocampal neural stem cells. By characterizing aging-associated shifts in transcription factor-associated regulatory features, the findings are intended to inform future studies aimed at preserving neural stem cell function during aging.

2. Materials and Methods

2.1 Reagents

DMEM-F12 cell culture medium, penicillin and streptomycin were obtained from Corning, and fetal bovine serum and penicillin/streptomycin were obtained from VWR. The primary V5-antibody was purchased from Abcam (SV5-PK1), and the secondary donkey anti-mouse Alexa 488-conjugated antibody was from Thermo Fisher Scientific (A21202).

2.2 ATAC-seq data acquisition and preprocessing

All genomic datasets were identified and downloaded from the Gene Expression Omnibus (GEO) repository (NCBI). Searches were performed using the keywords aging, hippocampus, neural stem cell, and ATAC-seq.

For hippocampal neural stem cell analyses, single-cell ATAC-seq data were obtained from GSE256417 (GSM8128515–GSM8128517), representing postnatal young (5 days), young adult (10 weeks), and old adult (24 weeks) mice. Peak sets were downloaded as author-provided scATACpeaks.bed.gz files. According to the original study, sequencing reads were aligned to the mm10 genome, quality-controlled, and peaks were called using the standard Cell Ranger and Signac/MACS2 pipeline. In the present study, only the processed peak coordinates were used; raw sequencing reads were not re-aligned or re-processed.

For whole-hippocampus aging and sex comparisons, ATAC-seq data from GSE244503 were analyzed. This dataset included male and female hippocampal samples from young (10-week) and aged (80-week) mice, with 6–8 biological replicates per group. As described by the original authors, reads were adapter-trimmed, aligned to mm10, filtered for blacklist and mitochondrial reads, and peaks were called using MACS2. Quality control metrics including TSS enrichment and FRiP scores were applied, and consensus peak sets were generated across replicates. In the present study, author-defined peak sets were used directly for motif enrichment analysis.

For subventricular zone neural stem cell analyses, ATAC-seq peak data were obtained from GSE214971 (GSM6619399–GSM6619404), consisting of three biological replicates each of young (2-month) and aged (18-month) mice. Peak coordinates were downloaded as author-processed bedgraph.gz files representing combined peak sets following

alignment, quality control, and peak calling in the original study.

Mouse ages were classified according to commonly used murine aging categories (neonatal/early postnatal <1 week; young adult 2–3 months; old adult 3–6 months; aged ≥18 months). The publicly available datasets analyzed here spanned multiple studies with distinct experimental designs and age sampling strategies; therefore, ages were not harmonized across datasets. Instead, analyses were performed within each dataset using the age groupings defined by the original studies, and results were interpreted as reflecting broad age-associated patterns rather than precisely matched chronological stages.

2.3 Motif finding analysis

All analyses were performed using author-provided, preprocessed ATAC-seq peak files aligned to the mm10 mouse genome, as deposited in GEO. Raw sequencing reads were not re-aligned or reprocessed. Bed or bedgraph files with chrom, chromStart, and chromEnd columns were first sorted by 'sort -k1,1 -k2,2n'. Peak regions called in 'O' but not in 'Y' samples were selected by running 'bedtools intersect -v -a O.bed -b Y.bed > O_specific_peaks.bed'. Output files were used as input to run HOMER (Hypergeometric Optimization of Motif EnRichment) algorithm (v5.1, 7-16-2024)(21) by 'findMotifsGenome.pl OvsY.bed mm10 homer_output/ -size given'. Motif enrichment was performed using HOMER with the default background model implemented by the software, which samples genomic regions matched for size and GC content from the mm10 genome. Reported p-values reflect nominal enrichment significance as computed by HOMER using a hypergeometric test. Although HOMER outputs both p-values and estimated false discovery rates (q-values), motif rankings and interpretation in this study were based on nominal p-values, and no additional multiple-testing correction was applied. Accordingly, motif enrichment results were treated as exploratory and descriptive rather than confirmatory.

2.4 Gene expression analysis

For hippocampal RNA sequencing (RNA-seq) datasets to compare old (4.5 month) and young neural stem cell gene expression profiles, GSE168031 series with GSM5124090 - GSM5124178 scRNA-seq datasets (48 vs. 41 cells of young [2 month] and aged [18 month]) were downloaded as normalized count values for comparison. Gene expression analyses were intended as descriptive support and did not employ replicate-aware statistical models optimized for scRNA-sequencing data. As such, these analyses did not account for zero inflation, cellular heterogeneity, or multiple-testing correction and were not used to draw definitive conclusions regarding differential expression. For subventricular zone neural stem cell expression analysis, GSE214971 series with GSM6544097 - GSM6544102 RNA-seq datasets (3 replicates of young [2 month] and aged [18 month]) were downloaded and plotted for descriptive comparison.

2.5 Cell culture

The human immortalized ReN VM neural progenitor cell line, originally obtained from Millipore Sigma (SCC008), was grown in DMEM-F12 medium supplemented with 1x B27 supplement, 10% fetal bovine serum and 1% streptomycin penicillin. The cells were

plated on fibronectin-coated well plates following dissociation by trypsin. While ReN VM cells cannot recapitulate aging mouse neural stem cells, these human cells were used due to the poor transfection efficiency of primary mouse neural stem cells.

2.6 Expression of MEF2C by transfecting plasmid

A culture of ReN cells was grown for the purpose of *in vitro* assay testing the effect of MEF2C overexpression on cellular contact. MEF2C plasmid DNA in the pInducer vector was introduced to cells by adding 5 micrograms of DNA mixed with 20 micrograms of polyethylenimine in OptiMEM serum-free media (Thermo Fisher Scientific). To induce the expression of MEF2C without causing acute stress and perturbation of cellular adhesion, doxycycline (0.2 micrograms/mL) was added to the media after cells were stably adhered and formed stable contact with the extracellular matrix and adjacent cells. Cells were allowed to express MEF2C for 72 hours. The culture was fixed by adding 4% paraformaldehyde.

2.7 Staining of cells and analysis of actin cytoskeleton

Fixed cells were permeabilized by treating them with 0.2% Triton-X100 in phosphate buffered saline (PBS) solution for 5 min. After two washes in PBS, anti-V5 antibody (Abcam SV5-PK1, 1:1,000 diluted) in 5% (W/V) bovine serum albumin in PBS was added and incubated for two hours. Following an additional two washes with PBS, secondary Alexa488 donkey anti-mouse IgG antibodies diluted in PBS were added to cells and incubated for one hour. Lastly, nuclei were stained by the addition of DAPI and the cytoskeleton was stained by the TRITC-phalloidin probe (Sigma-Aldrich P-1951, 1:1,000 dilution in PBS). The staining was visualized under the EVOS-FL auto microscope using a Texas red LED light cube for phalloidin, green fluorescence protein LED cube for V5, and DAPI blue cube for DNA. The percentage of nuclear V5 cells with contracted phalloidin staining was quantified manually from three independent 200x microscopic fields without blinding.

2.8 Quantitation and statistical analysis

The number of cells positive for V5 staining and showing round morphology without actin-positive contacts with neighboring cells was quantified manually and was used as a qualitative proxy for cell-cell contact. The results were normalized by dividing the number of V5-positive cells in an image. All results plotted were presented as mean ± standard deviation. For two group comparisons, a two-tailed unpaired Student t-test was applied to determine the significance of differences using GraphPad Prism software (version 7). Given the limited sampling and manual quantification, statistical testing was considered exploratory. $P < 0.05$ was used as a descriptive threshold.

3. Results

3.1 Analysis of age-associated ATAC-seq peak sets in hippocampal neural stem cells identifies enrichment of MEF2-family motifs

To address how age-associated changes in the chromatin landscape and related regulatory features were reflected in ATAC-seq peak patterns, publicly available datasets were selected from the NCBI Gene Expression Omnibus (GEO) using the keywords aging, hippocampus, neural stem cell, and ATAC-seq.

A dataset (GSM8128517) containing single-cell ATAC-seq data from hippocampal neural stem cells of 5-day-, 12-week-, and 24-week-old mice was analyzed. Preprocessed peak coordinate files aligned to the mm10 mouse genome were obtained from GEO and were used directly without reprocessing raw sequencing reads.

Peak files were sorted ('sort -k1,1 -k2,2n'), and peak intervals present in 24-week-old samples but not called in younger samples under the same preprocessing and peak-calling thresholds were identified using bedtools ('bedtools intersect -v'). Motif enrichment analysis was performed on these age-associated peak sets using HOMER (v5.1; (21) with the command 'findMotifsGenome.pl'. HOMER was run using its default background model, which samples genomic regions matched for size and GC content from the mm10 genome.

Motif enrichment significance was assessed using nominal p-values computed by HOMER via a hypergeometric test, and estimated false discovery rates (q-values) were also reported by the software. Motif rankings and interpretation in this study were based on nominal p-values. Accordingly, motif enrichment results were treated as descriptive, reflecting over-representation of sequence motifs within age-associated peak sets rather than evidence of transcription factor binding. Ranked motif results from pairwise comparisons are shown in Figures 1 and 2.

The analysis identified ATAC-seq peak intervals present in hippocampal neural stem cells from 24-week-old mice that were not called as peaks in 5-day- or 12-week-old samples under the applied preprocessing and peak-calling thresholds. Motif enrichment analysis of these age-associated peak sets identified sequence motifs corresponding to myocyte enhancer factor (MEF) family members, including MEF2C and MEF2D, among the top-ranked motifs (MEF2C, p-value = 1×10^{-839} and $1x\ 10^{-62}$ for 24-week vs. 5-day and 12-week comparisons, respectively; MEF2D, p-value = 1×10^{-1049} and 1×10^{-54} for the same comparisons).

Motif Name	Consensus	P-value	Log P-value	q-value
Mef2d(MADS)/Retina-Mef2d-ChIP-Seq(GSE61391)	GCTATTTTTAGC	1e-1049	-2.42E+03	0
Mef2c(MADS)/GM12878-Mef2c-ChIP-Seq(GSE32465)	DCYAAAAATAGM	1e-839	-1.93E+03	0
EBF(EBF)/proBcell-EBF-ChIP-Seq(GSE21978)	DGTCCCYRGGGA	1e-656	-1.51E+03	0
Mef2a(MADS)/HL1-Mef2a.biotin-ChIP-Seq(GSE21529)	CYAAAAATAG	1e-603	-1.39E+03	0
Ets1-distal(ETS)/CD4+-PolII-ChIP-Seq(Barski_et_al.)	MACAGGAAGT	1e-515	-1.19E+03	0
Mef2b(MADS)/HEK293-Mef2b.V5-ChIP-Seq(GSE67450)	GCTATTTTTGGM	1e-484	-1.12E+03	0
EBF2(EBF)/BrownAdipose-EBF2-ChIP-Seq(GSE97114)	NABTCCCWDGGGAVH	1e-418	-9.63E+02	0
NF1(CTF)/LNCAP-NF1-ChIP-Seq(Unpublished)	CYTGGCABNSTGCCAR	1e-401	-9.25E+02	0
Elk4(ETS)/Hela-Elk4-ChIP-Seq(GSE31477)	NRYTTCCGGY	1e-368	-8.48E+02	0
Elk1(ETS)/Hela-Elk1-ChIP-Seq(GSE31477)	HACTTCCGGY	1e-365	-8.42E+02	0

Figure 1. Top 10 ranked transcription factor binding motifs identified from the comparison of ATAC-seq peak sets in 24-week-old versus 5-day-old hippocampal neural stem cells. Motif enrichment analysis was performed using HOMER with 35,213 target sequences and 64,684 background sequences used for enrichment calculation. Numbers are presented in exponential notation.

Motif Name	Consensus Motif	P-value	Log P-value	q-value
Mef2c(MADS)/GM12878-Mef2c-ChIP-Seq(GSE32465)	DCYAAAAATAGM	1e-62	-1.44E+02	0
Mef2d(MADS)/Retina-Mef2d-ChIP-Seq(GSE61391)	GCTATTTTTAGC	1e-54	-1.26E+02	0
Ets1-distal(ETS)/CD4+-PolII-ChIP-Seq(Barski_et_al.)	MACAGGAAGT	1e-53	-1.22E+02	0
Fli1(ETS)/CD8-FLI-ChIP-Seq(GSE20898)	NRYTTCCGGH	1e-52	-1.21E+02	0
Etv2(ETS)/ES-ER71-ChIP-Seq(GSE59402)	NNAYTTCCTGHN	1e-51	-1.19E+02	0
Foxo3(Forkhead)/U2OS-Foxo3-ChIP-Seq(E-MTAB-2701)	DGTAAACA	1e-49	-1.13E+02	0
EBF(EBF)/proBcell-EBF-ChIP-Seq(GSE21978)	DGTCCCYRGGGA	1e-48	-1.11E+02	0
EBF2(EBF)/BrownAdipose-EBF2-ChIP-Seq(GSE97114)	NABTCCCWDGGGAVH	1e-48	-1.11E+02	0
Foxf1(Forkhead)/Lung-Foxf1-ChIP-Seq(GSE77951)	WWATRTAAACAN	1e-48	-1.11E+02	0
GABPA(ETS)/Jurkat-GABPa-ChIP-Seq(GSE17954)	RACCGGAAGT	1e-47	-1.10E+02	0

Figure 2. Top 10 ranked transcription factor binding motifs identified from the comparison of ATAC-seq peak sets in 24-week-old versus 12-week-old hippocampal neural stem cells. Motif enrichment analysis was performed using HOMER with 4,137 target sequences and 95,972 background sequences used for enrichment calculation. Numbers are presented in exponential notation.

Additional MEF2 paralogs, including MEF2A and MEF2B, were also identified with lower-ranked enrichment, consistent with shared sequence similarity among MEF2 family motifs. As a result, motif enrichment alone could not distinguish among MEF2 paralogs or infer transcription factor binding or protein-level activity. Accordingly, these findings were interpreted as identifying permissive sequence environments within age-associated peak sets rather than evidence of MEF2C- or MEF2D-specific regulatory activity.

Motif Name	Consensus Motif	P-value	Log P-value	q-value
NF1-halfsite(CTF)/LNCaP-NF1-ChIP-Seq(Unpublished)	YTGCCAAG	1e-471	-1.09E+03	0
CTCF(Zf)/CD4+-CTCF-ChIP-Seq(Barski_et_al.)	AYAGTGCCMYCTRGTGGCCA	1e-466	-1.07E+03	0
NF1(CTF)/LNCAP-NF1-ChIP-Seq(Unpublished)	CYTGGCABNSTGCCAR	1e-453	-1.04E+03	0
Atoh1(bHLH)/Cerebellum-Atoh1-ChIP-Seq(GSE22111)	VNRVCAGCTGGY	1e-406	-9.36E+02	0
Atoh7(bHLH)/Retina-Atoh7-CutnRun(GSE156756)	KRRCAGCTGGTS	1e-389	-8.97E+02	0
NeuroD1(bHLH)/Islet-NeuroD1-ChIP-Seq(GSE30298)	GCCATCTGTT	1e-333	-7.67E+02	0
BORIS(Zf)/K562-CTCFL-ChIP-Seq(GSE32465)	CNNBRGCGCCCCCTGSTGGC	1e-274	-6.31E+02	0
NeuroG2(bHLH)/Fibroblast-NeuroG2-ChIP-Seq(GSE75910)	ACCATCTGTT	1e-266	-6.13E+02	0
Lhx2(Homeobox)/HFSC-Lhx2-ChIP-Seq(GSE48068)	TAATTAGN	1e-243	-5.60E+02	0
Tlx(NR)/NPC-H3K4me1-ChIP-Seq(GSE16256)	CTGGCAGSCTGCCA	1e-240	-5.53E+02	0

Figure 3. Top 10 ranked transcription factor binding motifs identified from the comparison of ATAC-seq peak sets in 5-day-old versus 24-week-old hippocampal neural stem cells. Motif enrichment analysis was performed using HOMER with 42,231 target sequences and 56,752 background sequences used for enrichment calculation. Numbers are presented in exponential notation.

Next, ATAC-seq peaks selectively present in hippocampal neural stem cells from 5 day-old mice when compared to adult and old samples were filtered. These comparisons both showed enrichment of neurogenic transcription factor motifs such as NF1, NeuroD1, Atoh, Dlx, and

Lhx (Figures 3 and 4). These results suggested that the process of aging was associated with the suppression of neuronal cell fate genes, which may interfere with the differentiation of neural stem cells into newly generated neurons.

Motif Name	Consensus Motif	P-value	Log P-value	q-value
NF1-halfsite(CTF)/LNCaP-NF1-ChIP-Seq(Unpublished)	YTGCCAAG	1e-960	-2.21E+03	0
NeuroD1(bHLH)/Islet-NeuroD1-ChIP-Seq(GSE30298)	GCCATCTGTT	1e-732	-1.69E+03	0
Atoh1(bHLH)/Cerebellum-Atoh1-ChIP-Seq(GSE22111)	VNRVCAGCTGGY	1e-686	-1.58E+03	0
Dlx3(Homeobox)/Kerainocytes-Dlx3-ChIP-Seq(GSE89884)	NDGTAATTAC	1e-678	-1.56E+03	0
Lhx2(Homeobox)/HFSC-Lhx2-ChIP-Seq(GSE48068)	TAATTAGN	1e-672	-1.55E+03	0
DLX5(Homeobox)/BasalGanglia-Dlx5-ChIP-seq(GSE124936)	SSTAATTA	1e-668	-1.54E+03	0
Atoh7(bHLH)/Retina-Atoh7-CutnRun(GSE156756)	KRRCAGCTGGTS	1e-608	-1.40E+03	0
Lhx1(Homeobox)/EmbryoCarcinoma-Lhx1-ChIP-Seq(GSE70957)	NNYTAATTAR	1e-590	-1.36E+03	0
Gsx2(Homeobox)/LGE-Gsx2.Flag-ChIP-Seq(GSE162589)	CTAATTAGSN	1e-554	-1.28E+03	0
NF1(CTF)/LNCAP-NF1-ChIP-Seq(Unpublished)	CYTGGCABNSTGCCAR	1e-547	-1.26E+03	0

Figure 4. Top 10 ranked transcription factor binding motifs identified from the comparison of ATAC-seq peak sets in 12-week-old versus 24-week-old hippocampal neural stem cells. Motif enrichment analysis was performed using HOMER with 33,136 target sequences and 65,735 background sequences used for enrichment calculation. Numbers are presented in exponential notation.

3.2 Analysis of age-associated ATAC-seq peak sets in the aging hippocampus identifies enrichment of AP-1-associated motifs

Previous studies had reported the activation of stress-responsive AP-1 transcription factors across multiple human and mouse tissues, including the hippocampus (20). To assess whether similar motif enrichment patterns were observed in independent datasets, ATAC-seq data from the hippocampi of aging animals were analyzed using HOMER motif analysis. Potential sex-associated differences in aging-related motif enrichment were also examined, given the known influence of sex on hippocampal neurogenesis (22).

Motif Name	Consensus Motif	P-value	Log P-value	q-value
ZNF317(Zf)/HEK293-ZNF317.GFP-ChIP-Seq(GSE58341)	GTCWGCTGTYYCTCT	1e-12	-2.88E+01	0
NeuroG2(bHLH)/Fibroblast-NeuroG2-ChIP-Seq(GSE75910)	ACCATCTGTT	1e-8	-1.89E+01	0
Olig2(bHLH)/Neuron-Olig2-ChIP-Seq(GSE30882)	RCCATMTGTT	1e-7	-1.70E+01	0
Fra2(bZIP)/Striatum-Fra2-ChIP-Seq(GSE43429)	GGATGACTCATC	1e-6	-1.56E+01	0
JunB(bZIP)/DendriticCells-Junb-ChIP-Seq(GSE36099)	RATGASTCAT	1e-6	-1.44E+01	0.0001
Fra1(bZIP)/BT549-Fra1-ChIP-Seq(GSE46166)	NNATGASTCATH	1e-6	-1.44E+01	0.0001
Fos(bZIP)/TSC-Fos-ChIP-Seq(GSE110950)	NDATGASTCAYN	1e-6	-1.43E+01	0.0001
CTCF(Zf)/CD4+-CTCF-ChIP-Seq(Barski_et_al.)	AYAGTGCCMYCTRGTGGCCA	1e-5	-1.38E+01	0.0001
HOXA2(Homeobox)/mES-Hoxa2-ChIP-Seq(Donaldson)	GYCATCMATCAT	1e-5	-1.35E+01	0.0001
Fosl2(bZIP)/3T3L1-Fosl2-ChIP-Seq(GSE56872)	NATGASTCABNN	1e-5	-1.31E+01	0.0001

Figure 5. Top 10 ranked transcription factor binding motifs identified from the comparison of ATAC-seq peak sets in 80-week-old versus 10-week-old female mouse whole hippocampus. Motif enrichment analysis was performed using HOMER with 186 target sequences and 97,848 background sequences used for enrichment calculation.

Using the GSE244503 dataset, which compares hippocampal samples from adult (10-week) and aged (80-week) female and male mice (23), HOMER motif analysis ranked AP-1-associated motifs among the top enriched motifs in aged versus adult comparisons in both sexes, with nominal enrichment p-values on the order of 1 x 10^{-6} (Figures 5 and 6). In contrast, MEF2C- and MEF2D-associated motifs were not enriched in these whole hippocampal datasets.

Motif Name	Consensus Motif	P-value	Log P-value	q-value
CTCF(Zf)/CD4+-CTCF-ChIP-Seq(Barski_et_al.)	AYAGTGCCMYCTRGTGGCCA	1e-28	-6.52E+01	0
BORIS(Zf)/K562-CTCFL-ChIP-Seq(GSE32465)	CNNBRGCGCCCCCTGSTGGC	1e-19	-4.58E+01	0
Olig2(bHLH)/Neuron-Olig2-ChIP-Seq(GSE30882)	RCCATMTGTT	1e-9	-2.23E+01	0
ZNF317(Zf)/HEK293-ZNF317.GFP-ChIP-Seq(GSE58341)	GTCWGCTGTYYCTCT	1e-8	-2.05E+01	0
NeuroG2(bHLH)/Fibroblast-NeuroG2-ChIP-Seq(GSE75910)	ACCATCTGTT	1e-8	-2.03E+01	0
Atoh1(bHLH)/Cerebellum-Atoh1-ChIP-Seq(GSE22111)	VNRVCAGCTGGY	1e-8	-1.92E+01	0
AP-1(bZIP)/ThioMac-PU.1-ChIP-Seq(GSE21512)	VTGACTCATC	1e-6	-1.61E+01	0
Fos(bZIP)/TSC-Fos-ChIP-Seq(GSE110950)	NDATGASTCAYN	1e-6	-1.54E+01	0
Atf3(bZIP)/GBM-ATF3-ChIP-Seq(GSE33912)	DATGASTCATHN	1e-6	-1.53E+01	0
MyoD(bHLH)/Myotube-MyoD-ChIP-Seq(GSE21614)	RRCAGCTGYTSY	1e-6	-1.52E+01	0

Figure 6. Top 10 ranked transcription factor binding motifs identified from the comparison of ATAC-seq peak sets in 80-week-old versus 10-week-old male mouse whole hippocampus. Motif enrichment analysis was performed using HOMER with 366 target sequences and 97,763 background sequences used for enrichment calculation.

These findings were consistent with prior reports identifying AP-1 motif enrichment as a general feature of aging-associated chromatin landscapes across tissues. Importantly, replication of AP-1 enrichment in independent datasets was interpreted here as validation of broad aging-associated motif signatures rather than confirmation of MEF2C-specific findings. Differences in tissue composition, age definitions, and preprocessing pipelines across datasets may disproportionately affect detection of subtler motif signals, such as those associated with MEF2 family members. Accordingly, MEF2-related observations were interpreted cautiously and were restricted to neural stem cell-enriched datasets analyzed in this study.

3.3 Analysis of age-associated ATAC-seq peak sets in subventricular zone neural stem cells identifies enrichment of HOX-family motifs

There are two separate neurogenic regions in the mammalian brain: the hippocampus for excitatory neurons and the subventricular zone for inter-neurons (24). The function of subventricular zone-derived newborn neurons may not be directly relevant to aging-associated cognitive decline. It was hypothesized that the aging-associated enrichment of MEF2-family sequence motifs within ATAC-seq peak sets is specific to hippocampal neural stem cells but not those in the subventricular zone. To test this hypothesis, GSE214971 ATAC-seq data comparing young (2 month) and aged (18 month) subventricular neural stem cells were identified and analyzed using the same approaches described above.

As predicted, HOMER motif analysis of the GSE214971 ATAC-seq dataset identified entirely different sets of transcription factors,

showing newly gained accessibility in old subventricular zone neural stem cells. The most significant motif was HOXD13 (p-value=1 x 10^{-4}) together with motifs for other HOX family members (Figure 7). These results also indicate that MEF2C and MEF2D-associated sequence motifs are not enriched in age-associated ATAC-seq peak sets from subventricular zone neural stem cells. The findings from these three different datasets showed that cell type influences aging-associated motif enrichment patterns and gene expression changes.

Motif Name	Consensus Motif	P-value	Log P-value	q-value
Hoxd13(Homeobox)/ChickenMSG-Hoxd13.Flag-ChIP-Seq(GSE86088)	NCYAATAAAA	1e-4	-9.76E+00	0.027
Hoxd11(Homeobox)/ChickenMSG-Hoxd11.Flag-ChIP-Seq(GSE86088)	VGCCATAAAA	1e-3	-8.16E+00	0.067
Hoxa13(Homeobox)/ChickenMSG-Hoxa13.Flag-ChIP-Seq(GSE86088)	CYHATAAAAN	1e-3	-7.29E+00	0.107
HOXB13(Homeobox)/ProstateTumor-HOXB13-ChIP-Seq(GSE56288)	TTTTATKRGG	1e-3	-7.06E+00	0.107
Unknown(Homeobox)/Limb-p300-ChIP-Seq	SSCMATWAAA	1e-2	-6.09E+00	0.213
STAT1(Stat)/HelaS3-STAT1-ChIP-Seq(GSE12782)	NATTTCCNGGAAAT	1e-2	-6.02E+00	0.213
Hoxa11(Homeobox)/ChickenMSG-Hoxa11.Flag-ChIP-Seq(GSE86088)	TTTTATGGCM	1e-2	-5.62E+00	0.245
Hoxd10(Homeobox)/ChickenMSG-Hoxd10.Flag-ChIP-Seq(GSE86088)	GGCMATGAAA	1e-2	-5.51E+00	0.245
Zscan4c(Zf)/ESC-Zscan4c-ChIP-seq(GSE140619)	ATRTGTGCAC	1e-2	-5.48E+00	0.245
Phox2b(Homeobox)/CLBGA-PHOX2B-ChIP-Seq(GSE90683)	TTAATTNAATTA	1e-1	-4.37E+00	0.599

Figure 7. Top 10 ranked transcription factor binding motifs identified from the comparison of ATAC-seq peak sets in 18-month-old versus 2-month-old mouse subventricular zone neural stem cells. Motif enrichment analysis was performed using HOMER with 30 target sequences and 85,681 background sequences used for enrichment calculation. Numbers are presented in exponential notation.

3.4 Gene expression analysis of aging hippocampal neural stem cells shows increased MEF2C mRNA expression.

The enrichment of MEF2C- and MEF2D-associated motifs raises the possibility that differences in transcription factor expression may contribute to their representation in age-associated ATAC-seq peak sets. To explore whether transcript abundance differs with age, publicly available single-cell RNA-sequencing data comparing young and old subgranular zone hippocampal neural progenitors (GSE168031; (25)) were examined. Within this dataset, MEF2C mRNA levels were higher in older neural stem cell samples relative to younger ones, whereas MEF2D transcript levels did not show a comparable pattern (Figure 8). These observations did not establish transcription factor binding or activity but suggested that MEF2C expression may be associated with aging in hippocampal neural stem cells within the analyzed datasets.

MEF2C- and MEF2D-associated motifs were not among the age-associated motifs identified in subventricular zone neural stem cells (Figure 7). Consistent with this observation, analysis of a publicly available RNA-sequencing dataset comparing young (2 month) and aged (18 month) subventricular zone neural stem cells (GSE214971) did not reveal clear differences in MEF2C or MEF2D mRNA levels between age groups (Figure 9). These results did not support a strong age-associated change in MEF2C or MEF2D expression within the subventricular zone in the analyzed dataset.

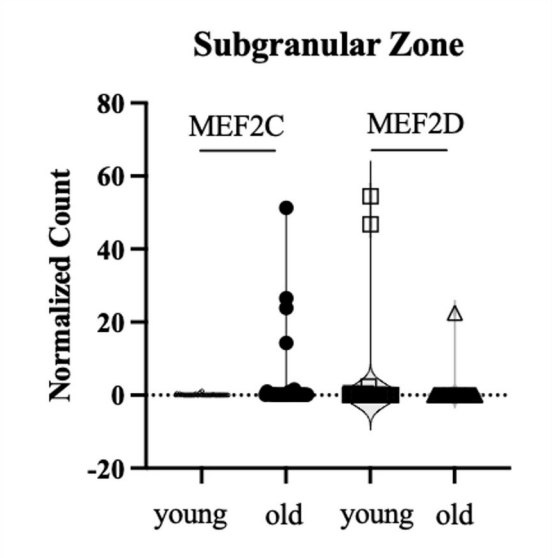

Figure 8. The normalized count for MEF2C/D from scRNA-seq data (GSE168031) of 5-month (old) vs. 2-month-old (young) mouse hippocampal neural stem cells. Violin plots show the distribution of normalized MEF2C expression across individual hippocampal neural stem cells (37 cells for old mouse and 42 cells for young mouse) in respective samples. Each point represents a single cell. Data are shown for descriptive and exploratory purposes only; no replicate-aware statistical inference is implied.

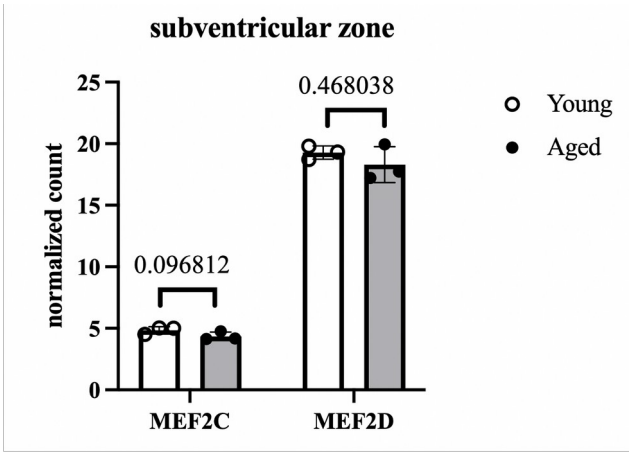

Figure 9. The normalized count for MEF2C/D from RNA-seq data of 18-month vs. 2-month-old mouse subventricular zone neural stem cells (3 mice per group). Unpaired two tailed Student t-test generated p-values are shown.

Taken together, these observations indicated that increased MEF2C mRNA expression was observed in hippocampal, but not subventricular zone, neural stem cell expression datasets examined in this study. One possible interpretation is that MEF2C motif enrichment

in age-associated hippocampal ATAC-seq peak sets may be associated with differences in MEF2C transcript abundance. However, motif enrichment alone does not establish transcription factor binding, activity, or regulatory function.

3.5 Introducing the expression of MEF2C in human neural progenitor-like cells reduces cell to cell contact

MEF2C has been reported to play a role in brain development by promoting neuronal differentiation. Previous studies have reported that MEF2C may regulate neuronal synapses by limiting excessive formation (26, 27). Based on these findings, it was hypothesized that increased MEF2C expression in aging neural stem cells may be associated with cellular features that influence interactions between neighboring cells. To explore this possibility in a simplified *in vitro* system, MEF2C was expressed by transfecting human MEF2C cDNA into the ReN VM human neural progenitor cell line. The MEF2C construct contained a V5 epitope tag, allowing detection of the expressed protein. Immunofluorescence staining confirmed nuclear localization of MEF2C-V5 (Figure 10, green), consistent with its expected subcellular distribution.

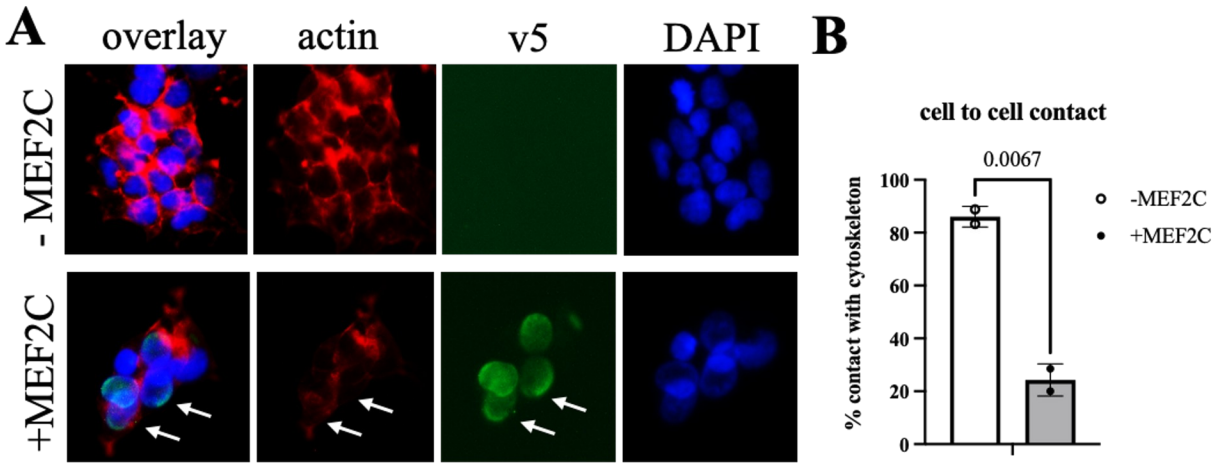

Figure 10. A. Representative fluorescence images of ReN cells either transfected to express MEF2C (+ doxycycline) or not (- doxycycline) for 72 hours. **B.** Quantitation of actin cytoskeleton rich cell-to-cell contacts from two independent experiments was quantified manually from three independent different 200x microscopic fields without blinding. Two tailed Student t-test was used for p-value. 200x images were acquired using EVOS FL Auto imaging software (v1.6).

Prior studies have reported MEF2C-associated transcriptional programs linked to reduced neuronal connectivity (26, 27). If increased MEF2C expression influences cellular interactions, cells with forced MEF2C expression might exhibit altered cell-cell contact. To assess this, actin cytoskeletal organization was examined in ReN cells with or without MEF2C expression. Actin structures were visualized using phalloidin conjugated to

Alexa 596, and MEF2C-expressing cells were identified by V5 immunostaining using Alexa 488. Cells expressing MEF2C-V5 displayed more rounded morphologies and reduced apparent contact with neighboring cells compared to non-transfected cells **(**Figure 10A). Quantification across multiple microscopic fields indicated a lower proportion of cells exhibiting actin-enriched contact regions in MEF2C-V5–expressing cells compared to controls (Figure 10B). Statistical testing was performed for exploratory purposes only.

These observations indicated that forced MEF2C expression was associated with altered cell morphology and reduced cell–cell contact in this *in vitro* system. However, this assay did not measure synapse formation, neuronal differentiation, or functional integration, and the observed morphological changes may reflect general cellular responses to transcription factor overexpression rather than specific regulatory effects on neuronal connectivity.

4. Discussion

In this study, age-associated differences in ATAC-seq peak landscapes were identified in hippocampal neural stem cells, accompanied by enrichment of MEF2-family sequence motifs within age-enriched peak sets. A central finding of this study is the cell-type specificity of aging-associated regulatory signatures. Although MEF2-family motif enrichment was identified in hippocampal neural stem cell peak sets, similar enrichment was not observed in whole hippocampal tissue or in subventricular zone neural stem cell datasets analyzed using comparable approaches. This contrast indicates that aging-associated regulatory features can be highly context-dependent and may be masked in bulk tissue analyses or differ across neurogenic niches. Together, these comparisons emphasize that cell identity strongly shapes the regulatory features associated with aging, and that conclusions drawn from one neural population may not generalize to others.

This study provides a cell-type-resolved view of aging-associated chromatin features by systematically comparing ATAC-seq peak-set motif enrichment across hippocampal neural stem cells, whole hippocampal tissue, and subventricular zone neural stem cells. Rather than identifying universal aging signatures, the analyses reveal that specific motif enrichments-exemplified by MEF2-family motifs-emerge selectively in hippocampal neural stem cell peak sets and are absent from bulk hippocampal tissue and other neurogenic niches. This selectivity demonstrates that aging-associated regulatory features are strongly context dependent and may be obscured in tissue-level analyses. Importantly, motif enrichment is interpreted as reflecting permissive regulatory sequence environments rather than transcription factor binding, activity, or causality, consistent with the peak presence-based nature of the analyses. Together, these findings establish that regulatory motif landscapes associated with aging are not uniform across brain regions or stem cell populations. The principal novelty of this work lies in defining cell-type specificity as a key dimension of aging-associated chromatin signatures, thereby providing a restrained, transparent framework for generating testable hypotheses in future mechanistic studies.

Motif enrichment analysis highlighted sequence motifs corresponding to both MEF2C and MEF2D among the top-ranked motifs in

hippocampal neural stem cell age-associated peak sets. When motif enrichment results were considered alongside publicly available gene expression data, MEF2C, but not MEF2D, showed higher mRNA expression in older hippocampal neural stem cell samples within the analyzed datasets. This distinction may reflect the high sequence similarity among MEF2 family motif matrices, which limits the ability of motif-based analyses to distinguish among paralogous transcription factors. Accordingly, motif enrichment alone cannot attribute regulatory activity to a specific MEF2 family member or establish transcription factor binding or function.

Previous studies had demonstrated roles for MEF2C in neuronal differentiation and lineage specification in cultured neural progenitors (28), and MEF2C depletion has been shown to impair neuronal differentiation. In contrast, the present study identified an association between increased MEF2C mRNA expression and enrichment of MEF2-associated sequence motifs in aging hippocampal neural stem cell datasets. These observations were correlative and do not establish a causal or functional role for MEF2C in age-related changes in neurogenesis.

One possible interpretation, informed by prior literature, is that MEF2C-associated regulatory states may be linked to cellular features related to neuronal morphology or connectivity. However, this interpretation remains speculative and was not directly tested in the present study. Importantly, age-associated declines in hippocampal neurogenesis may arise from multiple mechanisms, including altered proliferation, survival, or fate specification, rather than impaired synaptic integration alone.

To provide exploratory context, MEF2C was overexpressed in an immortalized human neural progenitor cell line that does not form functional synapses in culture. In this setting, actin cytoskeletal organization was used as a qualitative proxy for cell-cell contact rather than as a measure of synapse formation. Observed changes in cell morphology and contact are therefore interpreted as exploratory and do not demonstrate effects on synaptogenesis or neuronal integration. In addition, forced MEF2C overexpression may introduce non-physiological effects, including cellular stress. Future studies incorporating additional controls, such as DNA-binding-deficient MEF2C mutants (29), as well as *in vivo* perturbation approaches, will be required to more directly assess potential functional roles of MEF2C in neural stem cell aging.

Analysis of independent ATAC-seq datasets from whole hippocampal tissue revealed consistent enrichment of AP-1-associated motifs across age comparisons, in agreement with prior reports identifying AP-1 motifs as conserved aging-associated signatures across tissues (20, 30). Replication of AP-1 motif enrichment across heterogeneous datasets supports detection of general aging-associated regulatory features, while MEF2-associated findings are interpreted cautiously, given their greater sensitivity to dataset heterogeneity and preprocessing pipelines.

Across the datasets analyzed, similar sets of enriched transcription factor motifs were observed in comparisons between different age

groups. However, because these analyses rely on heterogeneous age groups, they do not establish trajectories of aging-associated regulatory change. Longitudinal or trajectory-based analyses would be required to determine whether observed patterns represent age-progressive states.

Finally, conclusions drawn here are limited to mouse hippocampal neural stem cells analyzed using publicly available datasets and an exploratory *in vitro* overexpression assay. These findings may not generalize to hippocampal aging broadly, other cell types, or functional cognitive outcomes. Instead, this study identifies candidate transcription factor-associated regulatory features linked to aging that may inform future, more mechanistic investigations.

5. Limitations

This study characterizes aging-associated regulatory features in hippocampal neural stem cells using motif enrichment of ATAC-seq peak sets from publicly available datasets. These limitations reflect a deliberately simple, peak-based approach focused on cell-type specificity rather than on transcription factor binding or causality. As a result, the analyses do not capture quantitative differences in chromatin accessibility or assess effect size, directionality, or reproducibility across replicates.

Motif enrichment analysis highlights permissive sequence environments associated with aging but does not establish transcription factor binding, occupancy, activity, or downstream gene regulation. In addition, sequence similarity among transcription factor family members, including MEF2 paralogs, limits attributing the results to a single factor. Accordingly, the findings are interpreted as associative and hypothesis-generating rather than evidence of defined regulatory programs or causal mechanisms.

The integration of heterogeneous public datasets spanning multiple age definitions and preprocessing pipelines provides broad coverage of aging-associated patterns but limits direct quantitative comparability. Replication of established aging signatures such as AP-1 motif enrichment supports detection of general aging features, while MEF2-associated findings are interpreted cautiously within this context.

Gene expression analyses and *in vitro* experiments were performed to provide complementary context. Expression analyses were descriptive, and functional assays relied on forced MEF2C expression in an immortalized human neural progenitor cell line, which does not model *in vivo* hippocampal neural stem cell aging or synapse formation. Observed changes in actin organization were therefore used as qualitative indicators of cell-cell contact and interpreted as exploratory.

Overall, the study identifies candidate transcription factor-associated regulatory features linked to aging while acknowledging that causal relationships and functional consequences will require future *in vivo* perturbation studies, direct binding assays, and longitudinal analyses.

6. Conclusion

Through this project, the study aimed to identify and characterize aging-associated transcriptional and chromatin features in the

hippocampus with the broader goal of informing future studies of neural stem cell aging. The identification of MEF2C-associated sequence motifs and increased MEF2C mRNA expression in aging hippocampal neural stem cells represents a novel association that may help guide subsequent mechanistic investigations.

The results of this analysis provide a framework that other researchers may build upon to further explore how transcription factor-associated regulatory features change during aging. However, translating these observations into strategies to preserve neural stem cell function will require substantial additional work, including quantitative chromatin analyses, direct measurements of transcription factor binding, and *in vivo* functional perturbations. A clearer understanding of MEF2C-associated regulatory states in aging hippocampal neural stem cells may ultimately contribute to efforts aimed at mitigating age-associated cognitive decline.

7. Acknowledgement

I am grateful to Dr. Tae-Wan Kim for his mentorship in molecular brain aging research, and to the researchers who made their datasets publicly available through the NCBI GEO database.

8. References

1. New Directions in the Sociology of Aging. In: Waite LJ, Plewes TJ, editors. New Directions in the Sociology of Aging. The National Academies Collection: Reports funded by National Institutes of Health. Washington (DC)2013.

2. Eriksson PS, Perfilieva E, Bjork-Eriksson T, Alborn AM, Nordborg C, Peterson DA, et al. Neurogenesis in the adult human hippocampus. Nature medicine. 1998;4(11):1313-7. https://doi.org/10.1038/3305

3. Altman J, Das GD. Autoradiographic and histological evidence of postnatal hippocampal neurogenesis in rats. J Comp Neurol. 1965;124(3):319-35. https://doi.org/10.1002/cne.901240303

4. Mu Y, Gage FH. Adult hippocampal neurogenesis and its role in Alzheimer's disease. Mol Neurodegener. 2011;6:85. https://doi.org/10.1186/1750-1326-6-85

5. Geigenmuller JN, Tari AR, Wisloff U, Walker TL. The relationship between adult hippocampal neurogenesis and cognitive impairment in Alzheimer's disease. Alzheimers Dement. 2024;20(10):7369-83. https://doi.org/10.1002/alz.14179

6. Aging NIo. Cognitive Health and Older Adults. 2024.https://www.nia.nih.gov/health/brain-health/cognitive-health-and-older-adults

7. Wu Y, Bottes S, Fisch R, Zehnder C, Cole JD, Pilz GA, et al. Chronic in vivo imaging defines age-dependent alterations of neurogenesis in the mouse hippocampus. Nat Aging. 2023;3(4):380-90. https://doi.org/10.1038/s43587-023-00370-9

8. Wrann CD, White JP, Salogiannnis J, Laznik-Bogoslavski D, Wu J, Ma D, et al. Exercise induces hippocampal BDNF through a PGC-1alpha/FNDC5 pathway. Cell Metab. 2013;18(5):649-59. https://doi.org/10.1016/j.cmet.2013.09.008

9. Erickson KI, Voss MW, Prakash RS, Basak C, Szabo A, Chaddock L, et al. Exercise training increases size of hippocampus and improves memory. Proc Natl Acad Sci. U S A. 2011;108(7):3017-22. https://doi.org/10.1073/pnas.1015950108

10. Farmand S, Du Preez A, Kim C, de Lucia C, Ruepp MD, Stubbs B, et al. Cognition on the move: Examining the role of physical exercise and neurogenesis in counteracting cognitive aging. Ageing Res Rev. 2025;107:102725. https://doi.org/10.1016/j.arr.2025.102725

11. Poulose SM, Miller MG, Scott T, Shukitt-Hale B. Nutritional Factors Affecting Adult Neurogenesis and Cognitive Function. Adv Nutr. 2017;8(6):804-11. https://doi.org/10.3945/an.117.016261

12. Cotman CW, Berchtold NC, Christie LA. Exercise builds brain health: key roles of growth factor cascades and inflammation. Trends Neurosci. 2007;30(9):464-72. https://doi.org/10.1016/j.tins.2007.06.011

13. Horvath S. DNA methylation age of human tissues and cell types. Genome Biol. 2013;14(10):R115. https://doi.org/10.1186/gb-2013-14-10-r115

14. Lu AT, Fei Z, Haghani A, Robeck TR, Zoller JA, Li CZ, et al. Universal DNA methylation age across mammalian tissues. Nat Aging. 2023;3(9):1144-66. https://doi.org/10.1038/s43587-023-00462-6

15. Stubbs TM, Bonder MJ, Stark AK, Krueger F, Team BIAC, von Meyenn F, et al. Multi-tissue DNA methylation age predictor in mouse. Genome Biol. 2017;18(1):68. https://doi.org/10.1186/s13059-017-1203-5

16. Itokawa N, Oshima M, Koide S, Takayama N, Kuribayashi W, Nakajima-Takagi Y, et al. Epigenetic traits inscribed in chromatin accessibility in aged hematopoietic stem cells. Nat Commun. 2022;13(1):2691. https://doi.org/10.1038/s41467-022-30440-2

17. Chen Y, Bravo JI, Son JM, Lee C, Benayoun BA. Remodeling of the H3 nucleosomal landscape during mouse aging. Transl Med Aging. 2020;4:22-31. https://doi.org/10.1016/j.tma.2019.12.003

18. Moskowitz DM, Zhang DW, Hu B, Le Saux S, Yanes RE, Ye Z, et al. Epigenomics of human CD8 T cell differentiation and aging. Sci Immunol. 2017;2(8). https://doi.org/10.1126/sciimmunol.aag0192

19. Bozukova M, Nikopoulou C, Kleinenkuhnen N, Grbavac D, Goetsch K, Tessarz P. Aging is associated with increased chromatin accessibility and reduced polymerase pausing in liver. Mol Syst Biol. 2022;18(9):e11002. https://doi.org/10.15252/msb.202211002

20. Patrick R, Naval-Sanchez M, Deshpande N, Huang Y, Zhang J, Chen X, et al. The activity of early-life gene regulatory elements is hijacked in aging through pervasive AP-1-linked chromatin opening. Cell Metab. 2024;36(8):1858-81 e23. https://doi.org/10.1016/j.cmet.2024.06.006

21. Heinz S, Benner C, Spann N, Bertolino E, Lin YC, Laslo P, et al. Simple combinations of lineage-determining transcription factors prime cis-regulatory elements required for macrophage and B cell identities. Mol Cell. 2010;38(4):576-89. https://doi.org/10.1016/j.molcel.2010.05.004

22. Yagi S, Splinter JEJ, Tai D, Wong S, Wen Y, Galea LAM. Sex Differences in Maturation and Attrition of Adult Neurogenesis in the Hippocampus. eNeuro. 2020;7(4). https://doi.org/10.1523/ENEURO.0468-19.2020

23. Achiro JM, Tao Y, Gao F, Lin CH, Watanabe M, Neumann S, et al. Aging differentially alters the transcriptome and landscape of chromatin accessibility in the male and female mouse hippocampus. Front Mol Neurosci. 2024;17:1334862. https://doi.org/10.3389/fnmol.2024.1334862

24. Jurkowski MP, Bettio L, E KW, Patten A, Yau SY, Gil-Mohapel J. Beyond the Hippocampus and the SVZ: Adult Neurogenesis Throughout the Brain. Front Cell Neurosci. 2020;14:576444. https://doi.org/10.3389/fncel.2020.576444

25. Ibrayeva A, Bay M, Pu E, Jorg DJ, Peng L, Jun H, et al. Early stem cell aging in the mature brain. Cell Stem Cell. 2021;28(5):955-66 e7. https://doi.org/10.1016/j.stem.2021.03.018

26. Barbosa AC, Kim MS, Ertunc M, Adachi M, Nelson ED, McAnally J, et al. MEF2C, a transcription factor that facilitates learning and memory by negative regulation of synapse numbers and function. Proc Natl Acad Sci. U S A. 2008;105(27):9391-6. https://doi.org/10.1073/pnas.0802679105

27. Flavell SW, Cowan CW, Kim TK, Greer PL, Lin Y, Paradis S, et al. Activity-dependent regulation of MEF2 transcription factors suppresses excitatory synapse number. Science. 2006;311(5763):1008-12. https://doi.org/10.1126/science.1122511

28. Cho EG, Zaremba JD, McKercher SR, Talantova M, Tu S, Masliah E, et al. MEF2C enhances dopaminergic neuron differentiation of human embryonic stem cells in a parkinsonian rat model. PLoS One. 2011;6(8):e24027. https://doi.org/10.1371/journal.pone.0024027

29. Molkentin JD, Black BL, Martin JF, Olson EN. Mutational analysis of the DNA binding, dimerization, and transcriptional activation domains of MEF2C. Mol Cell Biol. 1996;16(6):2627-36. https://doi.org/10.1128/MCB.16.6.2627

30. Karakaslar EO, Katiyar N, Hasham M, Youn A, Sharma S, Chung CH, et al. Transcriptional activation of Jun and Fos members of the AP-1 complex is a conserved signature of immune aging that contributes to inflammaging. Aging Cell. 2023;22(4):e13792. https://doi.org/10.1111/acel.13792